Cureus Journal of Engineering

Open Access Letter

Effect of Fe Doping on Dye Degradation of Calcium Titanate

Vikram U. Pandit [1] , Bhagwan D. Daphal [2] , Ganesh P. Jadhav [1]

1. Department of Chemistry, Haribhai V. Desai College, Pune, IND 2. Department of Chemistry, Modern College of Arts, Science & Commerce, Pune, IND

Corresponding author: Vikram U. Pandit, vikramupandit@gmail.com

Received 02/20/2025
Review began 03/03/2025
Review ended 04/19/2025
Published 04/29/2025

DOI:
https://doi.org/10.7759/s44388-025-03407-4

Abstract

In this study, a solid state process was used to synthesize Fe-doped $CaFe_xTi_{1-x}O_{3-\delta}$ with x = 0.05, 0.2, 0.5, 0.8, and 1.0. Characterization was done using X-Ray Diffraction, Diffuse Reflectance Spectra, and Tauc plot which confirms that the Fe substitution causes the band gap to move toward the visible portion of the spectrum in all produced materials. The degradation of Methylene Blue (MB) dye in sunlight was assessed for photocatalytic activity, considering the deleterious effects of complex, aromatic, and organic dyes. $CaTiO_3$ showed complete degradation of MB dye within 120 min of photocatalytic reaction time. Fe substitution is found to decrease the photocatalytic activity of $CaTiO_3$ unlike substitution in TiO_2 where photocatalytic activity has been reported to increase. We recommend this system and believe that this will open new era of materials synthesis and activity study.

Categories: Advanced Materials, Nano Materials, Water Resources Engineering
Keywords: doping, catio3, methylene blue, photocatalyst, industrial waste

Introduction

Aromatic complex organic dyes are used in the textile industry for many applications. Because of their complex nature, they remain in the water reservoirs for long periods of time, causing water pollution. Research interest in the photocatalytic degradation of organic dyes have increased swiftly in the last couple of decades, because about 15% of the global production of dyes is released from textile effluents [1]. This unused and toxic dye solution without treatment goes to groundwater leading to serious water contamination [2]. Many physical, chemical, and biological methods [3] are being researched for the cure of textile wastewater, but the search for a cost-effective and economical method still eludes the scientific society. Methylene Blue (MB) is a main class of dyestuffs resistant to biodegradation and is often used as a typical dye contaminant to evaluate the photocatalyst activity for many oxide-sulfide nanomaterials [4]. Photocatalysis is an economical and extensively used technique that can be utilized for the removal of pollutants from water [5].

Photocatalysis entails an inorganic or organic semiconductor photocatalyst with an appropriate band gap to produce charge carriers. These carriers are having a strong oxidizing and reducing potential, which in faith of redox reactions [6-8]. To date, TiO_2 is reported as a perfect catalyst, but it works only below 400 nm [9-11]. To utilize the solar spectrum effectively, a lot of research is going on to shift the band gap of TiO_2 close to or into the visible region by doping various anions and cations. $CaTiO_3$, one of the well-discussed wide band gap (Eg ~ 3.2 eV), is simple to synthesize, economical and very much stable material and has been evaluated in this work for its application as a photocatalyst [12-15]. Many reports are presented for the synthesis of $CaTiO_3$ using various methods. Recently, it has been reported that Fe-doped TiO_2 exhibits higher catalytic activity than pristine TiO_2 for the X-Ray Diffraction (XRD) dye in its aqueous solution [16,17].

The objective of the present work is to study the change in the band gap of $CaTiO_3$ toward the visible region with the help of Fe and to assess the effect of substitution on the photocatalytic activity toward MB degradation. This new product of oxide materials was evaluated for the impact of substitution on photocatalytic activity for degradation of MB. Based on our work experience in the nanomaterials field, photocatalysis, and organic chemistry, we believe that this work may be found suitable and useful for many other applications [18-21].

Materials And Methods

Statement of Problem: Developing new nanosystems with Ca metal and characterization of formed material systems for checking the photocatalytic MB dye degradation, considering its complex heterocyclic structure with the molecular formula $C_{16}H_{18}N_3SCl$.

Synthesis of Fe-doped $CaTiO_3$

How to cite this article
Pandit V U, Daphal B D, Jadhav G P (April 29, 2025) Effect of Fe Doping on Dye Degradation of Calcium Titanate . Cureus J Eng 2 : es44388-025-03407-4. DOI https://doi.org/10.7759/s44388-025-03407-4

For the experimental synthesis procedure, Fe-doped $CaTiO_3$ photocatalyst materials are described as follows. Fe-doped photocatalyst materials viz., $CaFe_xTi_{1-x}O_{3-\delta}$, where x = 0.05, 0.2, 0.5, 0.8, and 1.0, were synthesized with the help of the solid-state reaction method. Afterwards, the oxides of titanium (TiO_2) and iron (Fe_2O_3) were mixed thoroughly with a stoichiometric quantity of calcium carbonate and heated at 700°C for 48 h. This step led to the decomposition of calcium carbonate to its oxide. After cooling the reaction mixture to room temperature, this mixture was then ground properly followed by pelletization. Finally, this composition was heated at 900°C for 50 h. The last calcination step also involved occasional grinding, remixing, and pelletization for uniform photocatalyst synthesis.

Characterization

XRD (angle 10 to 70° range) technique (Philips PW 1820 Diffractometer, scan rate = 1°min -1) was used for identification of phases obtained for Fe-doped $CaTiO_3$ photocatalyst materials. The light absorbance characteristic of the catalysts was evaluated by a UV-Visible spectrometer (Shimadzu 1601) and the data obtained were used for band gap (range 200 nm-800 nm) evaluation of Fe-doped $CaTiO_3$ photocatalyst materials.

Photocatalytic activity study

The photocatalytic activity of as-synthesized $CaFe_xTi_{1-x}O_{3-\delta}$ photocatalyst was carried out under natural solar light. For all the photocatalysis experiments, 10 ppm aqueous MB dye solution was used for the study of the photocatalytic activity of the $CaFe_xTi_{1-x}O_{3-\delta}$ samples. A 1000 mL stock solution of 10 ppm MB was prepared by dissolving 10 mg of MB in distilled water in a volumetric flask. For the actual photocatalytic activity experiment, 100 ml 10 ppm MB solution was taken in a 150 mL conical flask. To this solution, 50 mg of as-prepared $CaFe_xTi_{1-x}O_{3-\delta}$ photocatalyst was added and stirred for 30 min without light to reach the equilibrium (adsorption desorption). After the equilibrium was reached, the solution was kept under sunlight with continuous stirring. After a fixed interval of time, a small volume (1-2 mL) of samples was taken and centrifuged for 15 min at 3000-3200 rpm to separate the catalyst ($CaFe_xTi_{1-x}O_{3-\delta}$). The supernatant liquid was analyzed using a UV-visible spectrophotometer to record the change in MB absorbance. The absorbance value at a wavelength of 665 nm was used to find out the % MB degradation. The % MB degradation was calculated using a general equation.

Results

Powder X-ray diffraction analysis

XRD patterns obtained for $CaFe_xTi_{1-x}O_{3-\delta}$ series of compositions, where $0 \leq x \leq 1$, are depicted in Figure *1*. The XRD pattern corresponding to $CaTiO_3$ (Figure *1a*) is found to match with its orthorhombic perovskite structure (JCPDS 42-0423). This crystal phase structure is retained up to 20 mole% Fe substitutions in the lattice (Figure *1b*) [19].

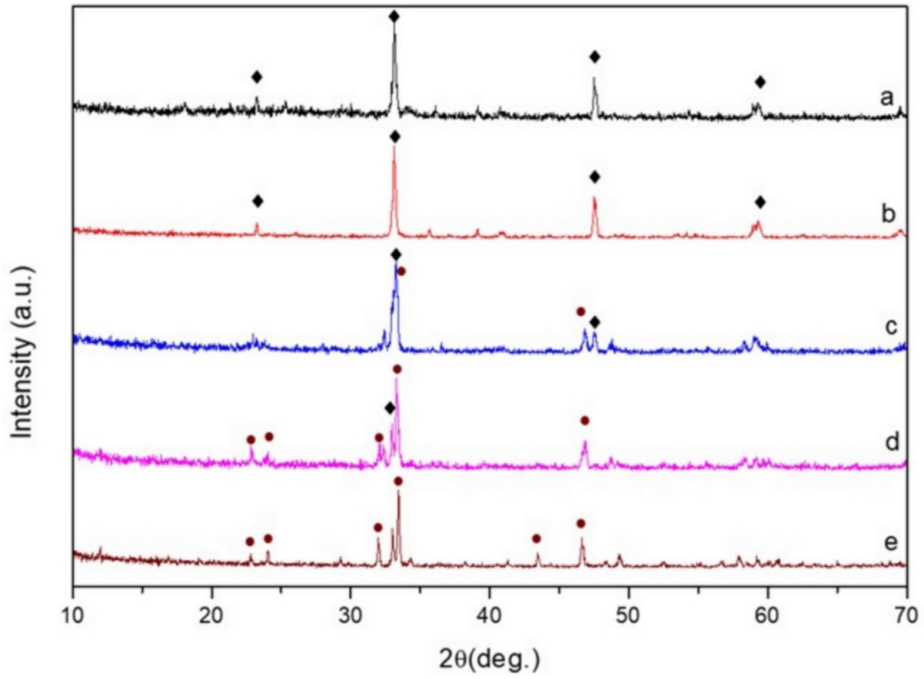

FIGURE 1: X-ray diffraction patterns of CaFexTi1-xO3-δ. (a) CaTiO3, (b) CaFe0.2Ti0.8O3, (c) CaFe0.5Ti0.5O3, (d) CaFe0.8Ti0.2O3, and (e) Ca2Fe2O5. (Filled diamonds) represent the CaTiO3 phase and (filled circles) represent Ca2Fe2O5

Whereas, the XRD pattern of the other extreme composition (Figure *1e*), where x = 1, confirm to match with orthorhombic $Ca_2Fe_2O_5$ (JCPDS 47-1744) phase. The other intermittent compositions are found to be a composite mixture of $Ca_3Fe_2TiO_8$ (JCPDS 30-0259) with $CaTiO_3$ or $Ca_2Fe_2O_5$ phases (Figure *1c* and d). The XRD pattern of $CaFe_{0.5}$ $Ti_{0.5}O_{3-\delta}$ (Figure *1c*) shows lines due to both $Ca_3Fe_2TiO_8$ and $CaTiO_3$. This phase distribution can be explained as per the following equation:

Whereas XRD results of $CaTi_{0.2}Fe_{0.8}O_{3-\delta}$ indicated that it is a mixture of $Ca_3Fe_2TiO_8$ and $Ca_2Fe_2O_5$ phases, formed as per following reaction:\(4 $CaCO_3$ + 2 TiO_2 + Fe_2O_3 → $Ca_3Fe_2TiO_8$ + $CaTiO_3$ + 4CO_2 ↑

5 $CaCO_3$ + TiO_2 + 2 Fe_2O_3 → $Ca_3Fe_2TiO_8$ + $Ca_2Fe_2O_5$ + 5CO_2 ↑\)

This clearly depicts that for substitution beyond 20 mole%, multi-phase systems exist, and their compositions depend on the stoichiometric ratio of the reactants used for synthesis.

Diffuse reflectance UV-visible spectroscopy

The Diffuse Reflectance Spectrum of $CaTiO_3$ shows the absorbance in the UV region with peaks at 322 and 276 nm. This composition depicts a sharp absorbance edge at 388 nm, corresponding to an energy band gap of 3.2 eV. The composition corresponding to 20 mole% substitution, having a single phase $CaTiO_3$ composition, depicts a similar absorbance profile, though with a weak shoulder at ~440 nm. The absorbance edge shifts to a higher wavelength, indicating the incorporation of Fe in the lattice structure of $CaTiO_3$. The other extreme composition corresponding to complete replacement of Ti by Fe, having the $Ca_2Fe_2O_5$ phase, depicts an absorbance profile consisting of two distinct peaks at 225 and 485 nm. The absorbance edge for this phase ($Ca_2Fe_2O_5$) is ~678 nm, corresponding to an energy band gap of 1.8 eV. The intermittent compositions consisting of the $Ca_3Fe_2TiO_8$ phase show extremely low absorbance (Figure *2*).

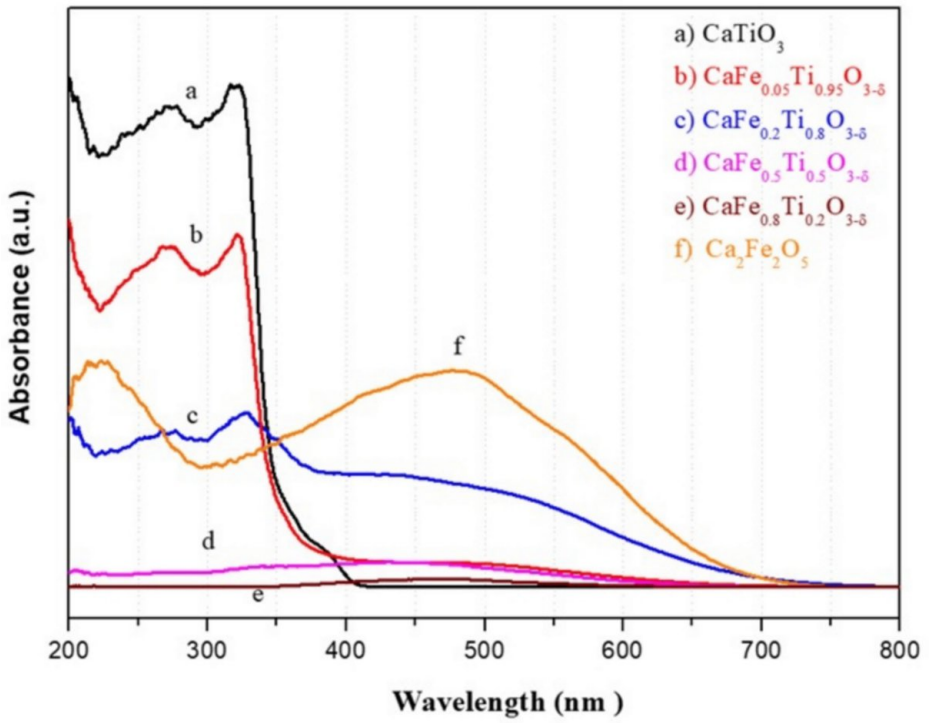

FIGURE 2: Diffuse reflectance UV-visible spectra of CaFexTi1-xO3-δ

Name of the compound	Phase identification by XRD	Lambda max. (nm)	Band gaps (eV)
$CaTiO_3$	$CaTiO_3$	276, 322	3.2
$CaFe_{0.05}Ti_{0.95}O_{3-\delta}$	$CaTiO_3$	276, 322	3.2
$CaFe_{0.2}Ti_{0.8}O_{3-\delta}$	$CaTiO_3$, $Ca_3Fe_2TiO_8$	276, 327, 440	1.8
$CaFe_{0.5}Ti_{0.5}O_{3-\delta}$	$Ca_3Fe_2TiO_8$, $CaTiO_3$	276, 340, 430	1.9
$Ca_2Fe_{0.8}Ti_{0.5}O_{3-\delta}$	$Ca_2Fe_2O_5$, $Ca_3Fe_2TiO_8$	468	2.0
$Ca_2Fe_2O_5$	$Ca_2Fe_2O_5$	225, 485	1.8

TABLE 1: Band gap analysis from diffuse reflection spectra of CaFexTi1-xO3-δ

XRD, X-Ray Diffraction

Overall, the absorbance profiles for $CaFe_xTi_{1-x}O_{3-\delta}$ series showed the decrease in absorbance in UV region with increasing extent of Fe substitution along with red shift in the absorbance edge. The calculated energy band gaps of $CaFe_xTi_{1-x}O_{3-\delta}$ series, where $0 \leq x \leq 1$, are listed in Table *1*.

Photocatalytic MB degradation study

Figure *3* illustrates UV-visible absorbance spectra of MB aqueous solution and change in its intensity on exposure to solar radiation, in the presence of pure $CaTiO_3$ photocatalyst.

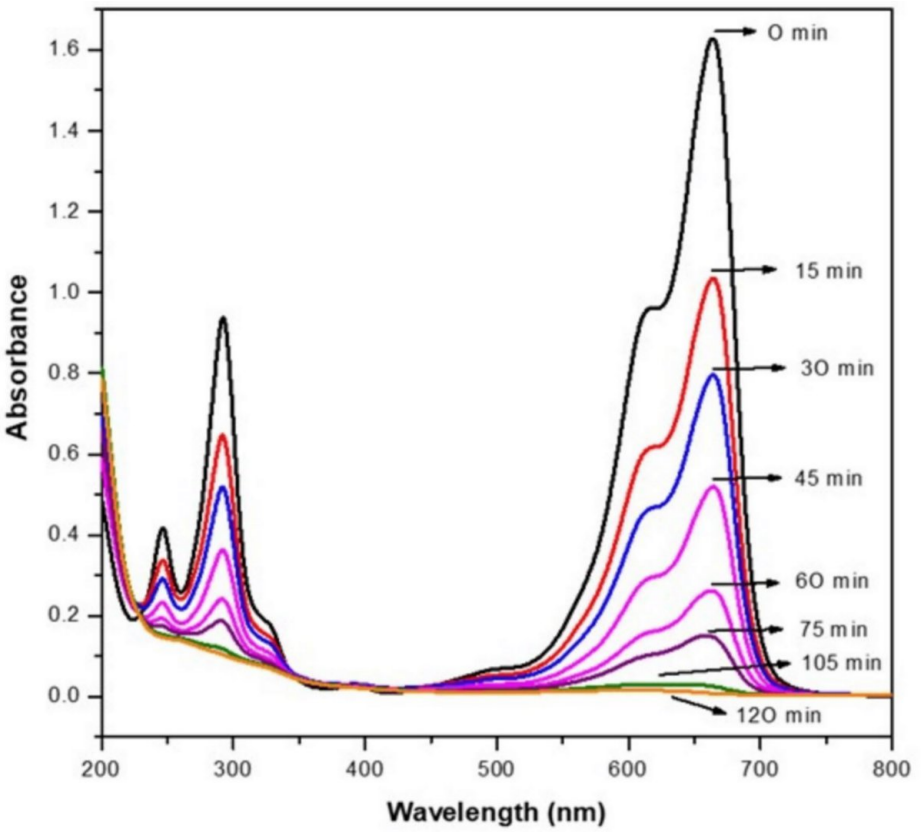

FIGURE 3: UV-visible spectra of MB degradation with CaTiO3 as catalyst under solar irradiation

MB, Methylene Blue

The main absorption peaks of MB are around 664, 617, 292, and 246 nm, which decrease gradually with increasing irradiation time during the photocatalytic experiment. The decomposition of MB dye in the presence of $CaTiO_3$ catalyst yields a colorless solution with no absorption at solar irradiation experiment time for 120 min. Data corresponding to the decrease in absorbance value for the 664 nm wavelength with time is plotted in Figure *4*, and a comparison is made for similar decrease for all the $CaFe_xTi_{1-x}O_{3-\delta}$ series catalysts. The rate for photocatalytic decay of MB on Fe substituted samples was found to be four times lower than that for pristine $CaTiO_3$. This might be due to the unavailability of the reaction sites in the formed catalysts' composition.

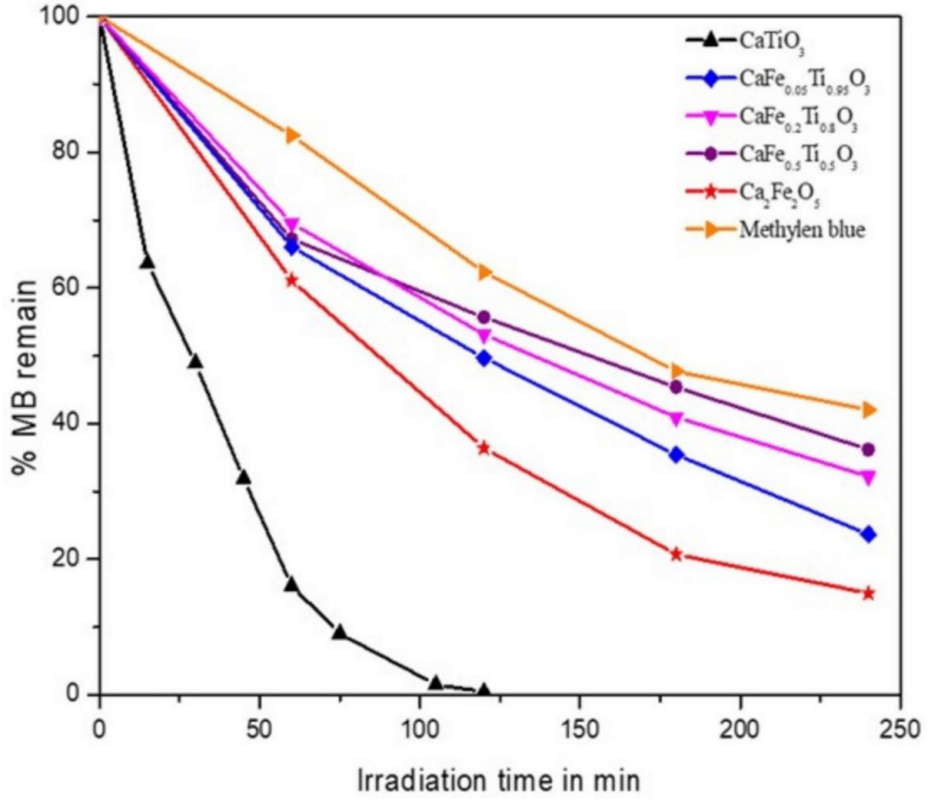

FIGURE 4: % MB degradation as a function of irradiation time

MB, Methylene Blue

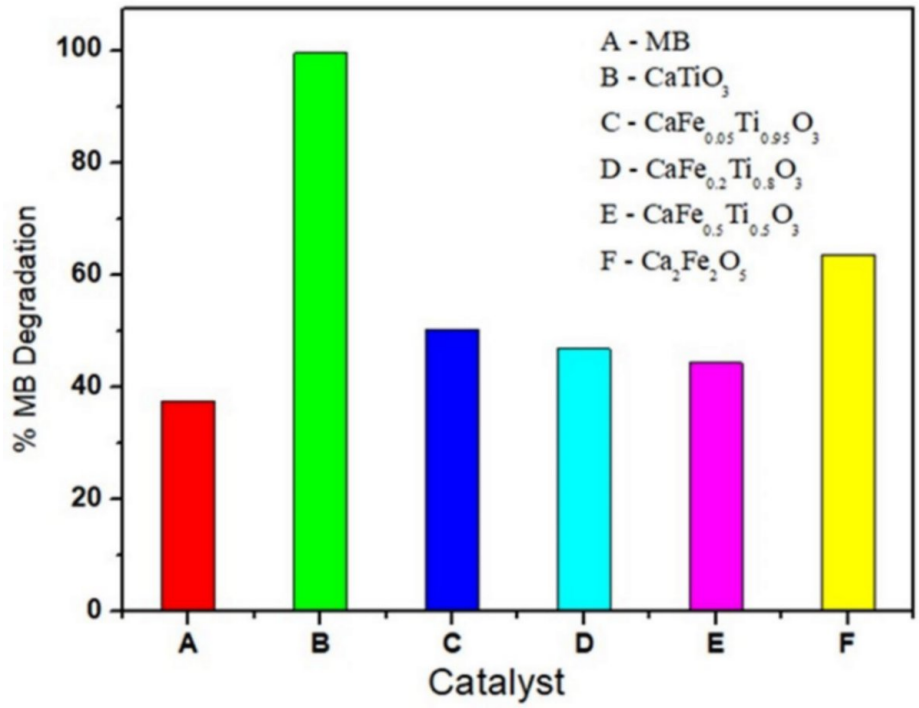

FIGURE 5: Comparison of MB degradation over different catalyst

MB, Methylene Blue

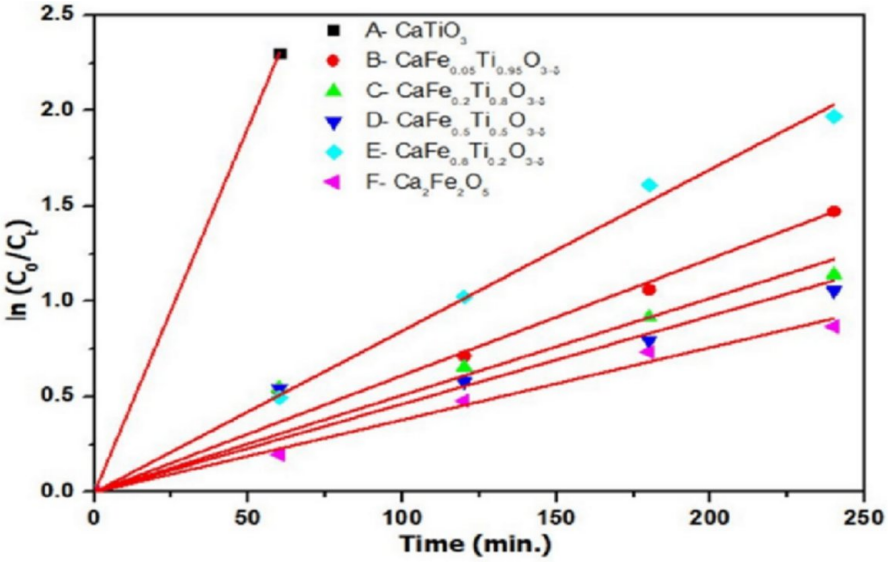

FIGURE 6: Kinetic study of photocatalysts

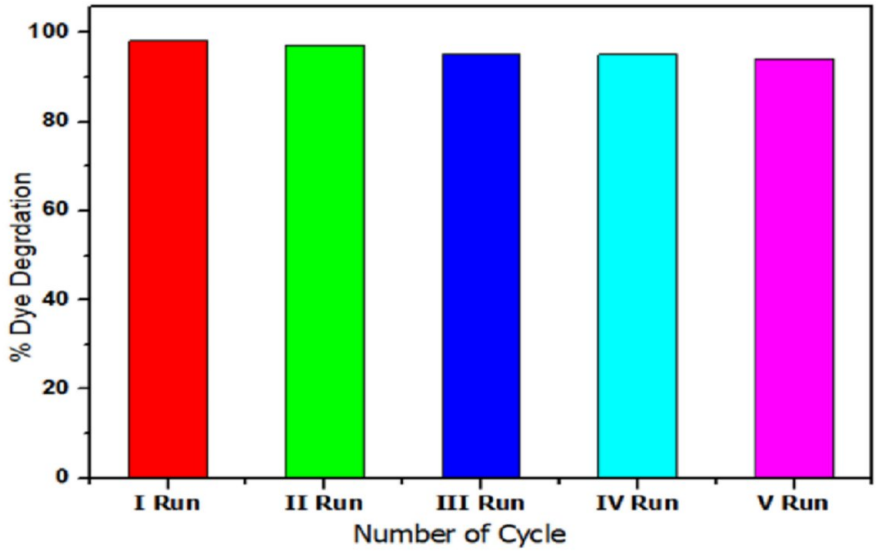

FIGURE 7: Recycle study of CaTiO3 towards MB dye degradation

MB, Methylene Blue

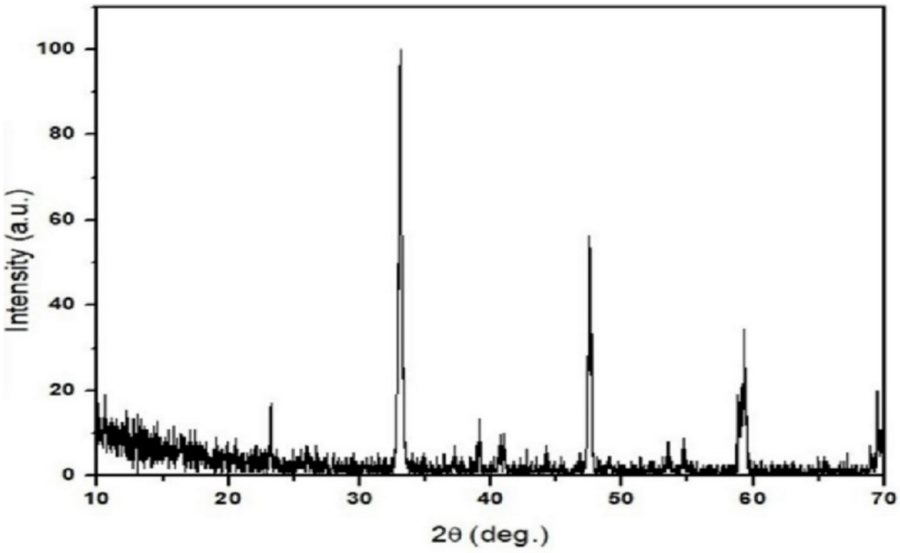

FIGURE 8: XRD of CaTiO3 after MB dye degradation

XRD, X-Ray Diffraction; MB, Methylene Blue

Discussion

This interpretation is clearly illustrated in Figure *5*, where the extent of MB degradation after 2 h is compared for all the photocatalysts of $CaFe_xTi_{1-x}O_{3-\delta}$ (x = 0, 0.05, 0.2, 0.5, 1) series. When Fe is substituted, the photocatalytic activity first declines but then rises once again with the final $Ca_2Fe_2O_5$ composition. The findings from DR UV-visible spectroscopy are in line with this pattern. According to the results, the existence of either the $CaTiO_3$ phase or the $Ca_2Fe_2O_5$ phase determines how effective these materials are as photocatalysts. This is contrary to earlier reported data for Fe-doped TiO_2, where an enhancement in photocatalytic activity was found to depend on the doping concentrations of Fe. For getting the rates of the dye degradation, kinetic plots are also given in the supporting information.

After plotting the kinetic study graphs, the rate constants (supporting information Figure *6*) for each photocatalyst are also provided in tabular format with standard error in Table *2*.

Sr. No.	Name of the Catalyst	Rate (Kapp) (min^{-1})	Standard Error
1	A-$CaTiO_3$	3.83x 10^{-2}	00
2	B-$CaFe_{0.05}$ $Ti_{0.95}O_{3-d}$	6.12x 10^{-3}	0.000248
3	C-$CaFe_{0.2}$ $Ti_{0.8}O_{3-d}$	5.09x 10^{-3}	0.000391
4	D-$CaFe_{0.5}$ $Ti_{0.5}O_{3-d}$	4.62x 10^{-3}	0.000420
5	E-$Ca_2Fe_{0.8}$ $Ti_{0.}O_{3-d}$	8.46x 10^{-3}	0.000164
6	F-MB	3.79x 10^{-2}	0.000116

TABLE 2: Kinetic study of Photocatalysts

In this study, it is observed that the catalytic conversion decreases with Fe substitution but then again increases for the final $Ca_2Fe_2O_5$ composition. This is in accordance with the data obtained from DR UV-visible spectra of these series of catalysts (Figure *2*). As is evident from that plot, the effectiveness of these materials as photocatalysts depends either on the presence of $CaTiO_3$ phase or $Ca_2Fe_2O_5$ phase. The third

phase of $Ca_3Fe_2TiO_8$ has very poor absorbance characteristics and hence makes no contribution to the absorbance profile, and hence its presence in the intermittent compositions is the cause for their poor photocatalytic activity. It can be concluded that Fe doping in $CaTiO_3$ exhibited lower catalytic activity as compared to both the parent $CaTiO_3$ and $Ca_2Fe_2O_5$ compositions due to the presence of third $Ca_3Fe_2TiO_8$ phase. Due to the problems of photocorrosion, many photocatalyst systems were found to be unstable toward the photocatalytic reactions. But, in this study for checking photostability of photocatalyst systems, we performed the recycle study for five cycles. Among the studied photocatalyst systems, $CaTiO_3$ showed the highest degradation activity so a recycle study is performed on $CaTiO_3$, and the results of this study are given in the supporting information Figure *7*.

Stability of $CaTiO_3$ was also confirmed by the post-dye degradation experiments with the help of XRD analysis. Figure *8* in the supporting information shows the similar XRD patterns as those before dye degradation experiments.

These formed photocatalyst systems might also be helpful for the degradation of colorless pollutants from the water.

Conclusions

When Fe is substituted for Ti in $CaTiO_3$ perovskite, several phasic systems are formed, which can include either the pristine $CaTiO_3$ or $Ca_2Fe_2O_5$ phases, or one of these phases combined with the $Ca_3Fe_2TiO_8$ phase. In comparison to extreme compositions, the diffuse reflectance UV-visible spectra of these catalyst series show a drop in mixed oxide absorbance as the $Ca_3Fe_2TiO_8$ phase grows, which also resulted in a decrease in mixed oxide catalysts' catalytic activity. Within 120 min of the photocatalytic reaction period, $CaTiO_3$ demonstrated full degradation of the MB dye. In contrast to substitution in TiO_2, where photocatalytic activity has been shown to increase, Fe substitution is found to lower the photocatalytic activity of $CaTiO_3$. Based on our expertise in organic chemistry, photocatalysis, and nanomaterials, we think this work could be appropriate and helpful for a wide range of other applications.

Additional Information

Author Contributions

All authors have reviewed the final version to be published and agreed to be accountable for all aspects of the work.

Concept and design: Vikram U. Pandit, Ganesh P. Jadhav, Bhagwan D. Daphal

Acquisition, analysis, or interpretation of data: Vikram U. Pandit

Drafting of the manuscript: Vikram U. Pandit, Ganesh P. Jadhav, Bhagwan D. Daphal

Critical review of the manuscript for important intellectual content: Vikram U. Pandit, Ganesh P. Jadhav

Supervision: Vikram U. Pandit

Disclosures

Human subjects: All authors have confirmed that this study did not involve human participants or tissue. **Animal subjects:** All authors have confirmed that this study did not involve animal subjects or tissue. **Conflicts of interest:** In compliance with the ICMJE uniform disclosure form, all authors declare the following: **Payment/services info:** All authors have declared that no financial support was received from any organization for the submitted work. **Financial relationships:** All authors have declared that they have no financial relationships at present or within the previous three years with any organizations that might have an interest in the submitted work. **Other relationships:** All authors have declared that there are no other relationships or activities that could appear to have influenced the submitted work.

References

1. Rafiq A, Ikram M, Ali S, Niaz F, Khan M, Khan Q, Maqbool M: Photocatalytic degradation of dyes using semiconductor photocatalysts to clean industrial water pollution. Journal of Industrial and Engineering Chemistry. 2021, 97:111-28. 10.1016/j.jiec.2021.02.017
2. Colmenares JC, Luque R: Heterogeneous photocatalytic nanomaterials: prospects and challenges in selective transformations of biomass-derived compounds. Chemical Society Reviews. 2014, 43:765-78. 10.1039/c3cs60262a
3. Singh KP, Gupta S, Kumar A, Mohan D: Multispecies QSAR modeling for predicting the aquatic toxicity of

diverse organic chemicals for regulatory toxicology. Chemical Research in Toxicology. 2014, 27:741-53. 10.1021/tx400371w

4. Harish S, Bharathia P, Prasada P, et al.: Interface enriched highly interlaced layered MoS2/NiS2 nanocomposites for the photocatalytic degradation of rhodamine B dye. RSC Advances. 2021, 11:19283-293. 10.1039/d1ra01941d
5. Schneider J, Matsuoka M, Takeuchi M, Zhang J, Horiuchi Y, Anpo M, Bahnemann DW: Understanding TiO2 photocatalysis: mechanisms and materials. Chemical Reviews. 2014, 114:9919-86. 10.1021/cr5001892
6. Jiang L, Yuan X, Pan Y, Liang J, Zeng G, Wu Z, Wang H: Doping of graphitic carbon nitride for photocatalysis: a review. Applied Catalysis B Environment and Energy. 2017, 217:388-406. 10.1016/j.apcatb.2017.06.003
7. Safajou H, Khojasteh H, Salavati-Niasari M, Mortazavi-Derazkola S: Enhanced photocatalytic degradation of dyes over graphene/Pd/TiO2 nanocomposites: TiO2 nanowires versus TiO2 nanoparticles. Journal of Colloid and Interface Science. 2017, 498:423-32. 10.1016/j.jcis.2017.03.078
8. Jawale V, Al-fahdawi A, Salve S, et al.: 6, 13-pentacenequinone/zinc oxide nanocomposites for organic dye degradation. Materials Today: Proceedings. 2022, 52:17-20. 10.1016/j.matpr.2021.10.098
9. Hao R, Wang G, Tang H, Sun L, Xu C, Han D: Template-free preparation of macro/mesoporous g-C3N4/TiO2 heterojunction photocatalysts with enhanced visible light photocatalytic activity. Applied Catalysis B Environment and Energy. 2016, 187:47-58. 10.1016/j.apcatb.2016.01.026
10. Kambur A, Pozan GS, Boz I: Preparation, characterization and photocatalytic activity of TiO2-ZrO2 binary oxide nanoparticles. Applied Catalysis B Environment and Energy. 2012, 115-116:149-58. 10.1016/j.apcatb.2011.12.012
11. Pandit VRU, Jadhav GKP, Jawale VMS, Dubepatil R, Gurao R, Late DJ: Synthesis and characterization of micro-/nano-α-Fe2O3 for photocatalytic dye degradation. RSC Advances. 2024, 14:29099-105. 10.1039/d4ra04575k
12. Passi M, Pal B: A review on CaTiO3 photocatalyst: activity enhancement methods and photocatalytic applications. Powder Technology. 2021, 388:274-304. 10.1016/j.powtec.2021.04.056
13. Cerón-Urbano L, Aguilar CJ, Diosa JE, Mosquera-Vargas E: Nanoparticles of the perovskite-structure CaTiO3 system: the synthesis, characterization, and evaluation of its photocatalytic capacity to degrade emerging pollutants. Nanomaterials. 2023, 13:2967. 10.3390/nano13222967
14. Zhao J, Cao X, Bai Y, Chen J, Zhang C: Simple synthesis of CaTiO3/g-C3N4 heterojunction for efficient photodegradation of methylene blue and levofloxacin. Optical Materials. 2023, 135:113239. 10.1016/j.optmat.2022.113239
15. García-Mendoza MF, Torres-Ricárdez R, Ramírez-Morales E, et al.: CaTiO3 perovskite synthetized by chemical route at low temperatures for application as a photocatalyst for the degradation of methylene blue. Journal of Materials Science Materials in Electronics. 2023, 34:1-11. 10.1007/s10854-023-10309-w
16. Zhu J, Zheng W, He B, Zhang J, Anpo M: Characterization of Fe-TiO2 photocatalysts synthesized by hydrothermal method and their photocatalytic reactivity for photodegradation of XRG dye diluted in water. Journal of Molecular Catalysis A: Chemical. 2004, 216:35-43. 10.1016/j.molcata.2004.01.008
17. Zhao H, Duan Y, Sun X: Synthesis and characterization of CaTiO3 particles with controlled shape and size. New Journal of Chemistry. 2013, 37:986-91. 10.1039/c3nj40974k
18. Singh A, Pandit VU, Sonawane SL: Bio-based raw materials for preparation of carbon nanostructures. Bio-derived Carbon Nanostructures. 2024, 25-63. 10.1016/B978-0-443-13579-8.00010-3
19. Demirors AF, Imhof A: BaTiO3, SrTiO3, CaTiO3, and BaxSr1-xTiO3 particles: a general approach for monodisperse colloidal perovskites. Chemistry of Materials. 2009, 21:3002-07. 10.1021/cm900693r
20. Pandit VU, Arbuj SS, Pandit SS, Gaikwad HK: Photocatalytic hydrogen production reactor system. MRS Communications. 2022, 12:1190-96. 10.1557/s43579-022-00292-4
21. Pandit VRU: Hydrogen as a clean energy source. Alternative Energies and Efficiency Evaluation. IntechOpen, 2022. 10.5772/intechopen.101536